






RESEARCH ARTICLE

10.1029/2024JG008286

Ecohydrological Variables Underlie Local Moisture Recycling in Mediterranean-Type Climates

Jolanda J. E. Theeuwen^{1,2} , Stefan C. Dekker¹ , Bert V. M. Hamelers^{2,3}, and Arie Staal¹ 

¹Copernicus Institute of Sustainable Development, Utrecht University, Utrecht, The Netherlands, ²Wetsus, European Centre of Excellence for Sustainable Water Technology, Leeuwarden, The Netherlands, ³Department of Environmental Technology, Wageningen University and Research, Wageningen, The Netherlands

Key Points:

- Local evaporation and precipitation recycling, and their underlying variables, vary among five Mediterranean regions globally
- Local evaporation and precipitation recycling correlate more with ecohydrological variables than with non-ecohydrological variables
- Local evaporation and precipitation recycling can possibly be used to find areas where land cover changes could enhance the local water cycle

Supporting Information:

Supporting Information may be found in the online version of this article.

Correspondence to:

J. J. E. Theeuwen,
j.j.e.theeuwen@uu.nl

Citation:

Theeuwen, J. J. E., Dekker, S. C., Hamelers, B. V. M., & Staal, A. (2024). Ecohydrological variables underlie local moisture recycling in Mediterranean-type climates. *Journal of Geophysical Research: Biogeosciences*, 129, e2024JG008286. <https://doi.org/10.1029/2024JG008286>

Received 4 JUN 2024

Accepted 24 SEP 2024

Author Contributions:

Conceptualization: Jolanda

J. E. Theeuwen, Stefan C. Dekker, Arie Staal

Formal analysis: Jolanda J. E. Theeuwen

Methodology: Jolanda J. E. Theeuwen, Stefan C. Dekker, Arie Staal

Supervision: Stefan C. Dekker, Bert V. M. Hamelers, Arie Staal

Visualization: Jolanda J. E. Theeuwen

Writing – original draft: Jolanda J. E. Theeuwen

Writing – review & editing: Stefan C. Dekker, Bert V. M. Hamelers, Arie Staal

Abstract Mediterranean areas are projected to face increased water scarcity due to global changes. Because a relatively large fraction of the precipitation in Mediterranean areas originates locally, changes at the land surface may further dampen local precipitation. Here, we study the contribution of evaporation to local precipitation for the first time on a scale of approximately 50 km using local evaporation recycling (ELMR) and local precipitation recycling (PLMR), and make a comparison among five Mediterranean climate regions: South West Australia, South West US, central Chile, the Mediterranean Basin, and the Cape region of South Africa. Specifically, this study aims to understand the effects of ecohydrological (dependent on vegetation or the hydrological cycle) and non-ecohydrological variables on ELMR and PLMR. We find that (a) on average, ecohydrological variables correlate more frequently and more strongly to ELMR and PLMR than non-ecohydrological variables; (b) ELMR is large over wet areas and PLMR is large over dry areas; and (c) there are differences in underlying factors of ELMR and PLMR among the regions due to differences in wetness, topography, and land cover. The results suggest that in Mediterranean regions, changes in vegetation cover or the hydrological cycle may strengthen the local water cycle through enhancing ELMR. Finally, ELMR and PLMR help to identify where in Mediterranean regions we might enhance the local water cycle through land cover changes.

Plain Language Summary In Mediterranean regions, an increase in evaporation may enhance rainfall locally, contributing to freshwater availability if the evaporation loss is compensated for by the additional rainfall. In this article we study this using two metrics that can provide insight into local rainfall. First, we analyze what fraction of evaporated water rains out within 50 km from where it is evaporated, which is called local evaporation recycling. Second, we analyze the fraction of rainfall that evaporated from within 50 km of where it rains out, which is local precipitation recycling. Although local evaporation and precipitation recycling are generally low, but can peak up to 10%, we find that variables related to vegetation and the hydrological cycle contribute to them. This suggests that specific changes in these variables might strengthen local recycling.

1. Introduction

Water scarcity is expected to increase across Mediterranean-type climate regions during the 21st century due to atmospheric warming (Lu et al., 2019). Globally, there are five major Mediterranean-type climate regions: South West Australia (SWA), South West US (SWUS), central Chile (CC), the Mediterranean Basin (MB), and the Cape region of South Africa (CSA). These regions are characterized by mild wet winters and warm dry summers (Lionello et al., 2006) and here, atmospheric warming exceeds global average rates, making them climate change hotspots (Ali et al., 2022). Previous studies on land–atmosphere feedbacks suggest that land cover changes, specifically greening, could be used to mitigate the intensification of extreme droughts and heatwaves and thus serve as a climate adaptation measure (e.g., Bonan, 2008; Miralles et al., 2019). For example, in the Mediterranean Basin, greening could compensate drying under future climate scenarios by increasing precipitation (Tuinenburg et al., 2022), but increased forest cover could also reduce streamflow due to increased evapotranspiration (Galleguillos et al., 2021), which we refer to as evaporation. Before we will be able to predict whether land cover changes could minimize drying locally, we first need to better understand the impacts of land cover on local precipitation.

Increased vegetation may contribute to precipitation (Baker, 2021; Cui et al., 2022; Spracklen et al., 2018) and atmospheric moisture recycling (Ellison et al., 2019; Layton & Ellison, 2016; Spracklen et al., 2012).

© 2024. The Author(s).

This is an open access article under the terms of the [Creative Commons Attribution License](https://creativecommons.org/licenses/by/4.0/), which permits use, distribution and reproduction in any medium, provided the original work is properly cited.

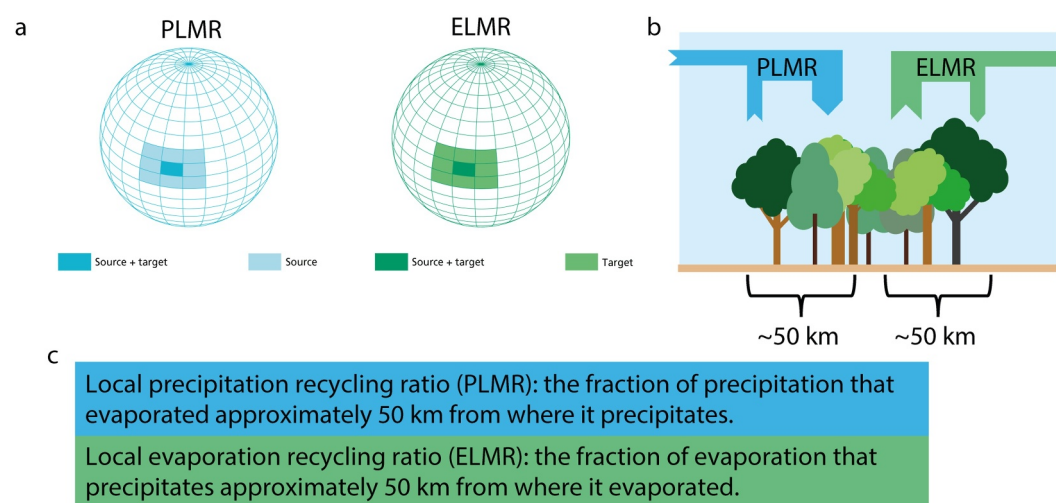


Figure 1. A schematic overview of (a) the calculation of local evaporation recycling and local precipitation recycling, (b) a visual representation of these processes in which the arrows indicate the moisture fluxes, and (c) their definition. Each grid cell has an area of $0.5^\circ \times 0.5^\circ$, however, the grids shown in panel (a) are on a different scale.

Atmospheric moisture recycling is the return of evaporated water as precipitation over land (Van der Ent et al., 2010), and is considered an ecosystem service (Keys et al., 2016). Moisture recycling can be calculated using atmospheric moisture connections between evaporation sources and precipitation sinks. For moisture connections over land, a change in an evaporation source, due to climate change or land cover change, can affect precipitation over land (Pranindita et al., 2022; Wang-Erlandsson et al., 2018). Therefore, moisture recycling may inform governance of land use to prevent depletion of water resources (Keys et al., 2017). Furthermore, the variability of moisture sources for specific regions can illustrate the vulnerability of precipitation to certain land cover changes, which is relevant for, for example, rainfed agricultural areas (Keys et al., 2012).

Basin recycling and regional recycling have been used to study rainfall effects of land cover within specific regions at spatial scales of several hundred kilometers or more (e.g., Staal et al., 2018; te Wierik et al., 2021; Wang-Erlandsson et al., 2018). Previous studies on source-sink relations could not isolate the more local effects of land cover on precipitation. Furthermore, studies on moisture recycling rarely focus on Mediterranean-type climate regions (te Wierik et al., 2021), despite their vulnerability to climate change. Therefore, in this study, we identify which landscape characteristics relate to local moisture recycling in Mediterranean regions. We separate landscape characteristics into ecohydrological and non-ecohydrological variables. Ecohydrological variables are directly related to vegetation or the hydrological cycle, and can therefore be altered through land cover changes; non-ecohydrological variables are not directly related to vegetation or the hydrological cycle. There are two indicators of recycling that allow us to study the local hydrological impacts of changes in evaporation. First, local evaporation recycling describes how much evaporated water returns as local precipitation; second, local precipitation recycling describes how much precipitation originated as local evaporation. By definition, local evaporation recycling does not directly depend on the influx of externally evaporated water whereas local precipitation recycling does.

To quantify local evaporation recycling, Theeuwes et al. (2023a) recently defined the local evaporation recycling ratio (ELMR) as the fraction of evaporation that returns within 0.5° as precipitation (Figure 1) using the output of an atmospheric moisture tracking model. Analogously, we here define the local precipitation recycling ratio (PLMR) as the precipitation equivalent of ELMR, that is, the fraction of precipitation that originates within 0.5° from its sink location (Figure 1). Although ELMR and PLMR conceptually resemble the regional recycling ratios developed by Van der Ent et al. (2010), regional recycling does not allow to study local processes, whereas local recycling does.

We aim to identify the relations ELMR and PLMR have with ecohydrological and non-ecohydrological variables in the five Mediterranean-type climate regions globally. This provides insight into how susceptible the local water

cycle is to land cover changes. Gaining insight into these relations is the first step in determining if and where land cover changes may enhance rainfall locally.

2. Methods

2.1. Atmospheric Moisture Recycling and Moisture Tracking

We study local moisture recycling using first, local evaporation recycling (ELMR), which is defined as the fraction of evaporated moisture that rains out within 0.5° from its source ($0.5 \times 0.5^\circ$) (Theeuwens et al., 2023a). On a grid, ELMR can be calculated as follows:

$$\text{ELMR} = \frac{\sum_{l=-1}^1 \sum_{k=-1}^1 P_{E,i+l,j+k}}{E_{ij}} \quad (1)$$

Here, E_{ij} is the total evaporation (tE) from the source grid cell and $P_{E,i+l,j+k}$ is the fraction of E_{ij} that rains out in the source grid cell and its eight neighboring grid cells. Second, we define and calculate the local precipitation recycling ratio (PLMR) as the fraction of precipitation that originates from within 0.5° from this sink location ($0.5^\circ \times 0.5^\circ$). On a grid, PLMR can be calculated as follows:

$$\text{PLMR} = \frac{\sum_{l=-1}^1 \sum_{k=-1}^1 E_{P,i+l,j+k}}{P_{ij}} \quad (2)$$

Here, P_{ij} is the total precipitation (tP) in the sink grid and $E_{P,i+l,j+k}$ is the fraction of this tP that evaporated from within this grid cell and its eight surrounding grid cells. Both ELMR and PLMR are determined for a single grid cell but dependent on moisture flows between that grid cell and its eight surrounding grid cells (Figure 1a). Regions with a similar latitude, such as the Mediterranean-type climate regions, have a similar grid cell size and thus, recycling is calculated over a constant surface area.

Both local recycling metrics are calculated with atmospheric moisture connections from evaporation source to precipitation sink from the data set by Tuinenburg et al. (2020b). These moisture connections are multi-year (2008–2017) monthly averages and have a spatial resolution of 0.5° . These data were calculated using the UTrack atmospheric moisture model, which is a Lagrangian moisture-tracking model (Tuinenburg & Staal, 2020). In this model, moisture parcels are released from each grid cell of 0.25° , which is currently the best available resolution for such a model. Within the grid cell, each mm of evaporation is represented by one hundred moisture parcels. These parcels are transported through the atmosphere by the wind in three dimensions. At each time step (0.1 hr), the moisture budget is made for each parcel. The evaporated moisture is randomly distributed over 25 vertical atmospheric levels according to the vertical moisture profile. Parcels are tracked for up to 30 days or up to the point at which only 1% of their original moisture is still present. Input data for evaporation, precipitation, precipitable water, and wind speed and direction were obtained from the ERA5 data set (Hersbach et al., 2020). We refer to Tuinenburg and Staal (2020) for a full description of the model, and to Tuinenburg et al. (2020b) for additional settings used for the data set.

We calculate multi-year (2008–2017) monthly averages of ELMR and PLMR at a spatial resolution of 0.5° , using the atmospheric moisture connections as input for Equations 1 and 2. To obtain multi-year seasonal averages and multi-year averages of ELMR and PLMR, we average ELMR weighted by the tE of each month in the source grid cell i, j , and we average PLMR weighted by the tP of each month in the sink grid cell i, j .

In addition to the local recycling ratios we also calculate the regional evaporation recycling ratio (ERMR) and regional precipitation recycling ratio (PRMR) for each of the five Mediterranean regions. We compare ERMR and PRMR with ELMR and PLMR to get insight into how local and regional patterns overlap or vary. ERMR is defined as the fraction of evaporated water from a specific study region that returns as rainfall within the same study region and PRMR is defined as the fraction of precipitation within a specific study region that originates as evaporation within that same study region. ERMR is calculated as follows:

$$\text{ERM}R = \frac{P_{E,\text{region}}}{E_{\text{region}}} \quad (3)$$

Here, E_{region} is the total amount of water that is evaporated from the study region and $P_{E,\text{region}}$ is the fraction of E_{region} that returns as rainfall to this study region. PRMR is calculated as follows:

$$\text{PRMR} = \frac{E_{P,\text{region}}}{P_{\text{region}}} \quad (4)$$

In this equation, P_{region} is the total amount of rainfall that falls within the study region and $E_{P,\text{region}}$ is the fraction of P_{region} that evaporated from within this study region.

2.2. Study Areas

Based on the Köppen climate classification (Peel et al., 2007), there are five major Mediterranean-type climate regions globally. We include all these terrestrial regions and some additional small terrestrial areas with a semi-arid climate to obtain five consecutive areas: South West Australia (SWA), South West US (SWUS), central Chile (CC), the Mediterranean Basin (MB) and the Cape region of South Africa (CSA) (Figure S1 in Supporting Information S1). These Mediterranean regions are found on both hemispheres between 30° and 40° latitude downwind from the ocean, which is typically on the western side of the continents (Lionello et al., 2006). The Mediterranean climate is characterized by dry and warm summers and wet and mild winters (Lionello et al., 2006). Annual precipitation varies between 250 and 1,200 mm, which falls predominantly in winter. Furthermore, the most important drivers of Mediterranean ecosystem functioning are climate, topography, soils and wildfire (Esler et al., 2018).

The five Mediterranean regions show differences in aridity and topography. For example, South West Australia and the Cape region of South Africa are relatively dry, with little rainfall and low aridity indices and South West US and central Chile are relatively wet (Table 1). Furthermore, all regions except for South West Australia include elevated terrain (Table 1). On average, for most regions, short vegetation cover is larger than tall vegetation except for the South West US where the tall vegetation cover is larger (Table 1). Finally, for all five regions, transpiration is the largest and most variable evaporation flux throughout the year. More detailed information per region is presented in Table 1. These data were obtained from ERA5 and ERA5-Land data, and were temporally and spatially averaged to obtain a multi-year (2008–2017) average of each variable for each region separately. More information about the data obtained from ERA5 and ERA5-Land data can be found in Section 2.3.

2.3. Ecohydrological and Non-Ecohydrological Variables

The main drivers of moisture recycling are in the interface between the land surface and atmosphere (Tuinenburg & Staal, 2020; Van der Ent et al., 2010): (a) horizontal wind speed, which transports the moisture away to remote locations; (b) precipitation, as it scales with the fraction of evaporated moisture that rains out locally; and (c) evaporation, as it affects the amount of water available for precipitation. Local moisture recycling could be affected by orography, distance to nearest coast, aridity, and vegetation (Shahidian et al., 2012; Theeuwes et al., 2023a; Tuinenburg et al., 2012; Vautard et al., 2010; Zurbenko & Luo, 2015).

We study the correlation between local recycling and 20 different variables. These variables are divided equally between ecohydrological and non-ecohydrological variables. Ecohydrological variables are directly related to vegetation or the hydrological cycle. Although we do not study the processes of land cover change specifically, these ecohydrological variables include some main processes that are affected by a change in vegetation. The ecohydrological variables (10) are: tP, tE, transpiration of vegetation (Evt), evaporation over bare soil (Ebs), evaporation over tree canopy (Etc), evaporation over open water (Eow), aridity index (AI), vapor pressure deficit (VPD), tall vegetation cover (≥ 3 m, vch), and short vegetation cover (vcl). The non-ecohydrological variables are (10): orography (z), zonal orography gradient (following latitude lines, dzdx), meridional orography gradient (following longitude lines, dzdy), zonal wind component at 10 and 100 m (u10 and u100), meridional wind component at 10 and 100 m (v10 and v100), total wind speed (V), wind direction ($\theta(V)$), and distance to the nearest coast (d).

Table 1
Characteristics of the Five Mediterranean Regions: South West Australia (SWA), South West US (SWUS), Central Chile (CC), the Mediterranean Basin (MB) and the Cape Region of South Africa (CSA)

	SWA	SWUS	CC	MB	CSA
Land surface area (# grid cells)	241	168	116	675	40
Average annual precipitation (mm)	360 (0.14)	1,060 (0.50)	800 (0.52)	650 (0.38)	390 (0.24)
Average annual evaporation:					
Total evaporation (mm)	551 (0.22)	470 (0.35)	552 (0.41)	535 (0.28)	381 (0.18)
Vegetation transpiration (mm)	174 (0.31)	256 (0.50)	249 (0.51)	302 (0.51)	228 (0.33)
Evaporation from tree canopy (mm)	59 (0.27)	88 (0.29)	52 (0.07)	75 (0.28)	62 (0.10)
Evaporation from bare soil (mm)	123 (0.11)	88 (0.33)	144 (0.40)	120 (0.33)	115 (0.16)
Evaporation from open water (mm)	20 (0.37)	17 (0.44)	5 (0.46)	16 (0.42)	20 (0.36)
Average vapor pressure deficit (hpa)	908 (0.44)	733 (0.51)	483 (0.45)	791 (0.58)	847 (0.30)
Average aridity index summer (-)	0.13	0.32	0.28	0.13	0.14
Average aridity index winter (-)	0.83	16	9.4	3.5	0.95
Average tall vegetation cover (-)	0.21	0.63	0.22	0.40	0.09
Average short vegetation cover (-)	0.75	0.31	0.65	0.49	0.86
Average elevation (m)	200	800	1,290	665	530
Max mountain peak (m)	465	2,657	3,692	2,417	1,010
Average wind speed (ms ⁻¹)	1.5 (0.35)	0.96 (0.23)	1.4 (0.15)	0.95 (0.24)	1.2 (0.29)

Note. This table shows spatial multi-year (2008–2017) averages calculated with data obtained from ERA5 and ERA5-Land. One grid cell is 0.5° (around 50 × 50 km). In-between brackets is the coefficient of variation over time which refers to annual variation and is defined as the ratio of the standard deviation over the annual average for the specific variable. Summer is defined as JJA for the Northern Hemisphere and DJF for the Southern Hemisphere. Winter is defined as DJF for the Northern Hemisphere and JJA for the Southern Hemisphere.

All data, except for the distance to the nearest coast, were obtained from or calculated with data from ERA5 or ERA5-Land. We used monthly averages for the years 2008–2017 of the ERA5 data (Hersbach et al., 2020) “on single levels” with a spatial resolution of 0.25° and ERA5-land data (Muñoz-Sabater et al., 2021) with a spatial resolution of 0.1° to calculate multi-year seasonal averages. As atmospheric moisture recycling has a temporal scale of up to several weeks, we study seasonal averages to understand which processes underlying LMR are important throughout the year. The gradient of orography in zonal and meridional directions, AI, VPD and wind direction and magnitude were calculated using ERA5 data. All data were centrally averaged to obtain a spatial resolution of 0.5°.

As ERA5 data do not include the different evaporation fluxes we used ERA5-Land to quantify these. This leads to some discrepancies in the evaporation balance. We find that tE is not always equal to the sum of the separate evaporation fluxes. This could be due to different model settings. However, the two products are internally consistent.

Furthermore, we obtained the variable “distance to nearest coast” from NASA (downloaded from: <https://oceancolor.gsfc.nasa.gov/docs/distfromcoast/>) (NASA, 2012) with an original spatial resolution of 0.01°. We centrally averaged the data spatially to obtain a resolution of 0.5°.

2.4. Statistical Methods

Spearman rank correlation is used to quantify the correlation between the local recycling metrics and each variable separately; principal component analysis (PCA) (Abdi & Williams, 2010; Bro & Smilde, 2014) is used to validate the results of the Spearman rank correlation and to study the clustering of ecohydrological and non-ecohydrological variables (i.e., covariance). For PCA, clustering is based on the angle between the loading of two variables. A more detailed description of PCA is presented in Text S1 in Supporting Information S1. We calculated the correlation coefficients and conducted the PCA using data for each region on 0.5° resolution for 10-

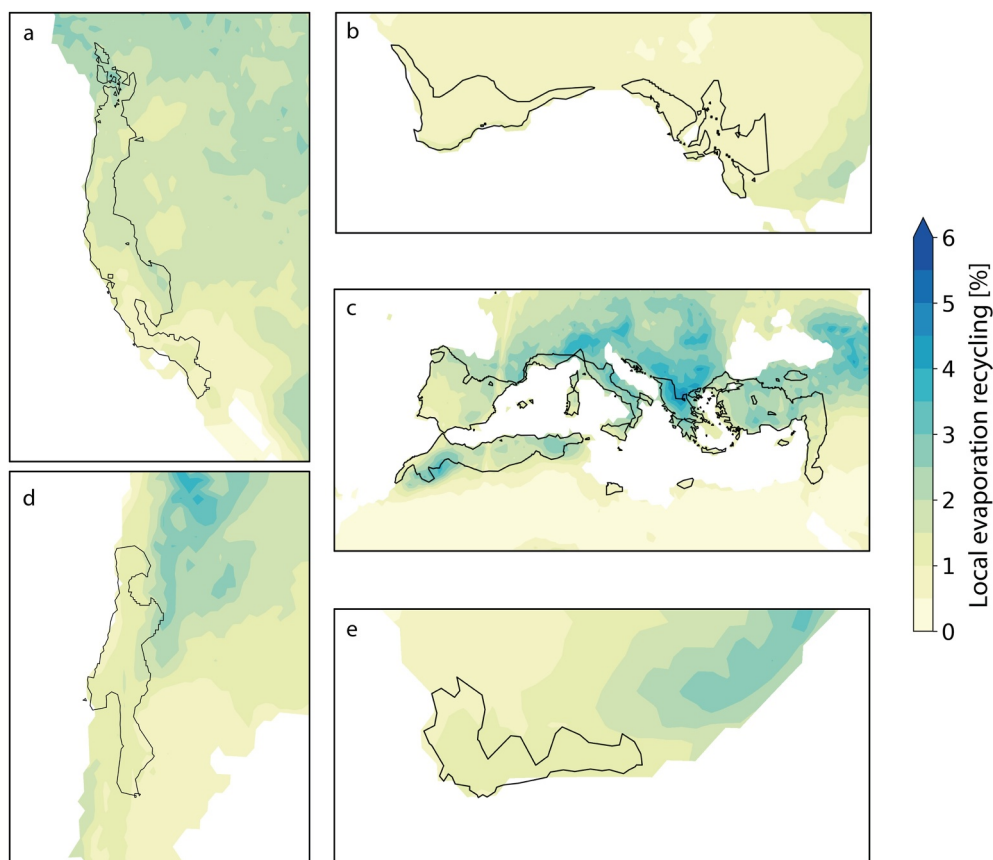


Figure 2. The multi-year (2008–2017) average of ELMR at a spatial resolution of 0.5° in all Mediterranean regions: (a) South West US, (b) South West Australia, (c) Mediterranean Basin, (d) central Chile, and (e) the Cape region of South Africa. The outlined areas indicate the study regions.

year averages (2008–2017) for every season and year. Combining these two statistical methods allows us to study one-on-one monotonic (both linear and nonlinear) relations with the Spearman rank correlation method as well as multivariate linear correlations with the PCA. We hereby study the nonlinearities in the Earth system and how they can be affected by multiple processes. The Python packages *scipy-stats* and *scikit-learn* were used to conduct the analyses. Finally, we use the *NumPy* package to calculate the maximum recycling ratios for each region.

3. Results

3.1. Spatio-Temporal Variation in Moisture Recycling

3.1.1. Local Evaporation Recycling and Local Precipitation Recycling

For each Mediterranean area, ELMR, which is the evaporated moisture that returns as precipitation to its source location, is on average, 1%–2% (Figure 2). Furthermore, PLMR, which is the fraction of precipitation that originates locally (within 50 km from this sink location), is also on average 1%–2% (Figure 3), across all Mediterranean areas. A large spatial variation in the annual ELMR and PLMR is found over elevated areas and maximum recycling ratios are obtained over mountain peaks (Figures 2 and 3). In South West Australia, the driest region of all, the annual averaged ELMR is exceptionally small ($<1\%$) compared to the other four regions (Figure S2 in Supporting Information S1). In the South West US and central Chile, the regions with the highest annual precipitation, PLMR is small on average ($<1\%$) compared to the other regions (Figure S2 in Supporting Information S1), indicating the large contribution of water that evaporated externally. The highest annually averaged ELMR and PLMR are found for the Mediterranean Basin ($>4\%$).

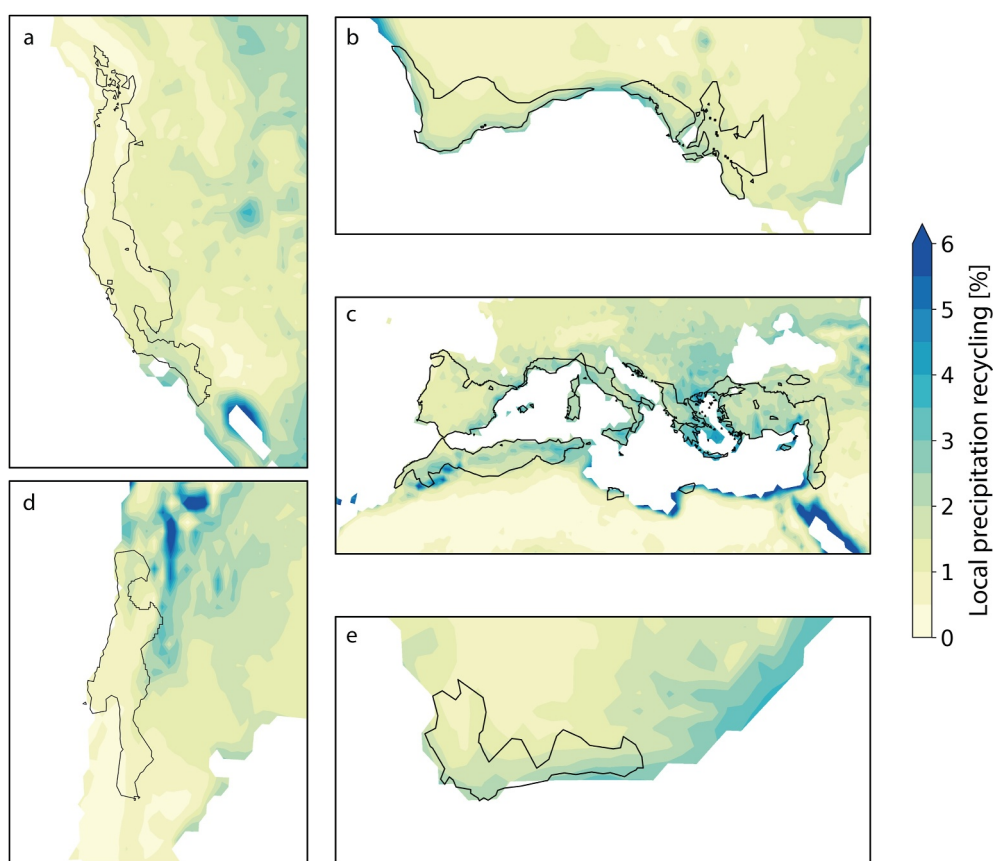


Figure 3. The multi-year (2008–2017) average of PLMR at a spatial resolution of 0.5° in all Mediterranean regions: (a) South West US, (b) South West Australia, (c) Mediterranean Basin, (d) central Chile, and (e) the Cape region of South Africa. The outlined areas indicate the study regions.

Furthermore, for all regions, PLMR and ELMR are highest during summer (JJA on Northern Hemisphere and DJF on the Southern Hemisphere) and lowest during winter. For some regions, the difference between summer and winter is larger, which is the case for the Mediterranean Basin, than for other regions, such as South West Australia. However, for all regions the seasonal pattern of PLMR is stronger than the pattern of ELMR (Figures 4a and 4b). Especially for the Mediterranean Basin, there is a strong variation in the spatial mean of PLMR throughout the year, with a peak ($>11\%$) in summer (Figure 4b). Peaks in the spatial mean of ELMR throughout the year are less distinct (Figure 4a). For the Mediterranean Basin the relatively high maxima in ELMR across the region (Figure 2) are canceled out by large areas with a very low ELMR. Similarly, we find differences in the spatial variation among the Mediterranean-type climate regions (Figures 4c and 4d and Figure S2 in Supporting Information S1). Throughout the year, the spatial variation in ELMR and PLMR is largest for the Mediterranean Basin and smallest for South West Australia (Figure S2 in Supporting Information S1). Especially during summer, PLMR can become relatively large in some grid cells compared to the mean value, even exceeding 15% (Figure 4d). Such high values are not observed for ELMR.

3.1.2. Regional Evaporation Recycling and Regional Precipitation Recycling

Similar to ELMR and PLMR, regional evaporation recycling (ERMR) and regional precipitation recycling (PRMR) vary among the five Mediterranean regions and are highest in the Mediterranean Basin, the largest Mediterranean region. Here, on average, 18.9% of evaporation returns as precipitation within the region and 16.2% of precipitation originates from within the region (Table S1 in Supporting Information S1). Furthermore, for South West US and central Chile, ERMR decreases and PRMR increases with increasing distance to the coast (Figures S3 and S4 in Supporting Information S1). For the Mediterranean Basin, PRMR increases toward the eastern side of the Basin. Finally, contrasting with ELMR and PLMR, both ERMR and PRMR are smallest for the

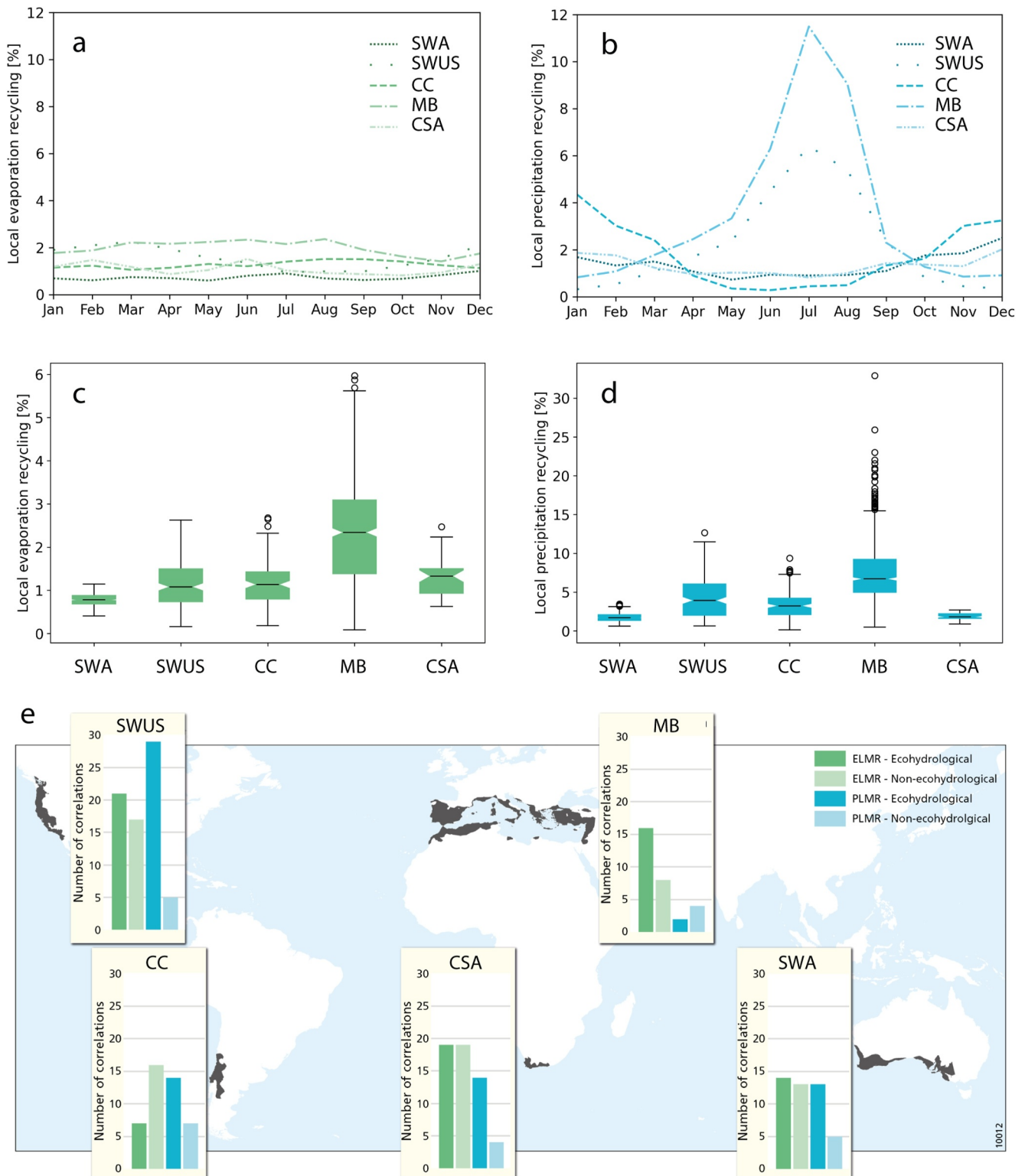


Figure 4.

Cape region in South Africa (both are 2.9%), which is the smallest Mediterranean region (Figures S3 and S4 & Table S1 in Supporting Information S1).

3.2. Correlations Between Local Moisture Recycling and Ecohydrological and Non-Ecohydrological Variables

In this section we describe the results that are most relevant to determine how ELMR and PLMR relate to ecohydrological and non-ecohydrological variables. We refer to Text S2 and S3, Figures S5–S10, and Tables S2–S8 in Supporting Information S1 for a more detailed description of the results.

3.2.1. Monotonic, Univariate Correlations

The number of significant moderate to strong correlations between ELMR/PLMR and ecohydrological/non-ecohydrological variables obtained from the Spearman rank correlation is plotted per region (Figure 4e). For all regions, except central Chile, there are more significant correlations between ELMR and ecohydrological variables than between ELMR and non-ecohydrological variables. We find a similar result for PLMR, which correlates most with ecohydrological variables in all regions, except for the Mediterranean Basin. A detailed description of the number of significant correlations per region and season is presented in Tables 2 and 3 and described in Text S2 in Supporting Information S1.

ELMR correlates most with variables related to wetness (i.e., tP, AI and VPD), specifically tP, and wind speed (Table 2). However, it is not solely dependent on these variables, given that ELMR is highest in the Mediterranean Basin, which is not the wettest region. This high ELMR is instead likely caused by the complex topography of the Mediterranean Basin. PLMR correlates most (both positive correlations and negative correlations) with evaporation over tree canopy and VPD (Table 3), followed by tE and distance to the coast. Different from the Spearman rank correlation, the PCA indicates that the evaporation fluxes related to vegetation also play an important role for ELMR, in two of the study regions. Temporal patterns in the correlation coefficients vary among the regions, as well as between ELMR and PLMR. For example, some variables correlate with ELMR throughout the year, such as the ecohydrological variables for South West US and the Mediterranean Basin and the non-ecohydrological variables for central Chile. During summer specifically, ELMR correlates with a relatively large number of variables. For PLMR, this peak in the number of correlations is not as clearly observed, despite its clear seasonality. Generally, correlations between ecohydrological variables and ELMR are consistent with correlations between ecohydrological variables and PLMR, that is, moderate to strong positive correlations for ELMR do not co-occur with strong negative correlations with PLMR for the same variables, and vice versa. However, for the South West US, we do observe such inconsistencies for precipitation, AI and VPD.

Finally, both ELMR and PLMR also have insignificant correlation coefficients for all regions (Tables 2 and 3). The Cape region of South Africa has a large number of insignificant correlations for both ELMR and PLMR, which may be explained by the small sample size of this region. Furthermore, for central Chile, ELMR has many insignificant correlations with ecohydrological variables compared to non-ecohydrological variables, suggesting the dependence of ELMR on the latter. Through similar reasoning we find that, for the South West US, ELMR seems to depend more on ecohydrological variables and for both the South West US and Mediterranean Basin, PLMR seems to depend more on the ecohydrological variables.

3.2.2. Linear, Multivariate Correlations: Clustering of Variables

To complement the Spearman rank correlations, the PCA gives insight into the clustering of the ecohydrological and non-ecohydrological variables (Figures S5–S10 and Tables S3–S8 in Supporting Information S1). For the average of all regions, there are 11 sets of ecohydrological variables, and two sets of non-ecohydrological

Figure 4. Differences in ELMR and PLMR among the five major Mediterranean-type climate regions for the period 2008–2017. SWUS: South West US, MB: Mediterranean Basin, CC: central Chile, CSA: the Cape region of South Africa, SWA: South West Australia. (a) Variation of ELMR throughout the year, where the values are averages over the 10-year period and all grid cells of that specific region. (b) Variation of PLMR throughout the year, similar to (a). (c) Boxplots indicating the distribution of ELMR for all grid cells in each region during summer (JJA on the Northern Hemisphere and DJF on the Southern Hemisphere). The values are 10-year seasonal averages. The green box indicates the interquartile range, and the black horizontal line in this box indicates the median value of ELMR. (d) Boxplots indicating the distribution of PLMR for all grid cells during summer, similar to (c). (e) The number of moderate to strong ($\rho \geq 0.4$) significant correlations between either PLMR/ELMR and ecohydrological/non-ecohydrological variables.

Table 2
Significant ($p < 0.05$) Correlation Coefficients for Spearman Rank Correlation (ρ_s) Between ELMR and Ecohydrological and Non-Ecohydrological Variables for Five Mediterranean Regions and All Seasons

	South West Australia			South West US			Central Chile			Mediterranean Basin			Cape region of South Africa			
	DJF	MAM	JJA	DJF	MAM	JJA	DJF	MAM	JJA	DJF	MAM	JJA	DJF	MAM	JJA	SON
Ecohydrological variables																
tp	0.41	0.26	0.64	0.61	0.60	0.31	0.27	0.40	0.58	0.55	0.68	0.43	0.87	0.42	0.74	0.59
tE	-0.15	0.25	0.52	0.52	0.28	0.16	0.20	0.23	-0.22	0.20	0.17	0.26	0.35	0.39	0.67	0.36
Evt	0.46	0.61	0.61	0.25	0.29	0.29			-0.18	0.31	0.32	0.42	0.69	0.57	0.62	0.33
Ebs	0.27	-0.33	-0.19	-0.81	0.67	0.55	0.30	-0.20	-0.52	-0.26	0.53		0.67	0.59	0.58	0.58
Etc	0.25	0.34	0.55	0.63	0.43	0.48	0.43		0.38	0.38	-0.20	0.41	0.67	0.59	0.58	0.58
Eow			0.29	0.14	0.16				0.12		-0.20		0.76	0.74	0.48	0.48
AI	0.29	0.38	0.59	0.65	0.82	0.78	0.58	0.60	0.65	0.56	0.61	0.42	0.76	0.74	0.48	0.48
VPD	-0.18	-0.40	-0.33	-0.68	-0.77	-0.71	-0.26	-0.64	-0.43	-0.46	-0.13	-0.51	-0.49	-0.38	-0.68	-0.41
vch	0.32	0.39	0.33	0.33	0.57	0.56	0.28	0.24	-0.08	0.08	0.23	0.13	0.49	0.60	0.48	0.48
vcl	-0.26		-0.46	-0.32	-0.23	-0.26					-0.12	-0.14				
Non-ecohydrological variables																
z	0.40	-0.47		0.22	0.69	0.59		0.36	0.09	0.32	0.38	0.20	0.44	-0.74	-0.58	0.66
dzdx	-0.43		0.24		-0.26	-0.26	0.30	0.30	0.13				0.52	0.61		
dzdy	0.28	0.22			0.39	0.21	-0.36	0.26	0.27	0.23	-0.10		0.70	0.66	-0.63	-0.69
u10	-0.44	0.49		0.29	-0.46	-0.39	-0.52	-0.48	-0.73	-0.40	-0.45	-0.17	-0.70		-0.64	-0.71
u100	-0.42	0.50		0.35	-0.36	-0.32	-0.51	-0.42	-0.76	-0.39	-0.43	-0.15	-0.66		0.41	0.39
v10	-0.53		-0.26	-0.45	-0.55	-0.24	0.32		0.18	0.27	0.10	0.17		0.41	0.39	0.39
v100	-0.59		-0.30	-0.42	-0.59	-0.24	0.24		0.18	0.32	0.12	0.23		0.41	0.39	0.39
V	-0.02	-0.34	0.16	-0.23	-0.59	-0.47	-0.46	-0.47	-0.40	-0.49	-0.58	-0.26	0.67	0.40	-0.36	0.62
θ(V)	0.52		-0.27	-0.24	-0.59	-0.47		-0.21	0.14	0.23	-0.19	0.23	0.67	0.40	-0.36	0.62
d		0.51	0.13	0.19	-0.56	-0.36	0.35	-0.20	0.14	0.23	-0.19	0.23	0.67	0.40	-0.36	0.62

Note. The color indicates a positive (red) or negative (blue), and a strong (dark) or weak (light) correlation. Empty cells represent insignificant correlations. Coefficients larger than 0.4 are embolded. tp: total precipitation; tE: total evaporation; Evt: evaporation from tree canopy; Ebs: evaporation from bare soil; Etc: evaporation from open water; AI: Aridity index; VPD: vapor pressure deficit; vch: vegetation cover tall vegetation; vcl: vegetation cover short vegetation; z: orography; dzdx: zonal orography gradient; dzdy: meridional orography gradient; u10: zonal wind at 10 m; u100: zonal wind at 100 m; v10: meridional wind at 10 m; v100: meridional wind at 100 m; V: total wind speed; θ(V): wind direction; and d: distance to nearest coast.

Table 3
Significant ($p < 0.05$) Correlation Coefficients for Spearman Rank Correlation (ρ_s) Between PLMR and Ecohydrological and Non-Ecohydrological Variables for Five Mediterranean Regions and All Seasons

	South West Australia			South West US			Central Chile			Mediterranean Basin			Cape region of South Africa				
	DJF	MAM	JJA	DJF	MAM	JJA	DJF	MAM	JJA	DJF	MAM	JJA	DJF	MAM	JJA	SON	
Ecohydrological variables																	
tp	-0.35	0.14	0.16	0.23	-0.62	-0.91	-0.75	-0.85	-0.33	-0.36	-0.62	-0.66	-0.20	-0.36	-0.27	0.46	
te	0.68	0.56	0.41	0.62	0.68	-0.23	-0.37	-0.53	-0.34	-0.34	0.66	0.39	0.51	-0.15	0.24	0.67	
Evt	0.40			0.53	0.42		-0.47	-0.66	-0.32	0.39	0.30	0.30	0.37	-0.11		0.63	
Ebs	-0.55			-0.47	0.76	0.79	-0.41	0.62	0.40	0.66	0.28	0.28	0.08	-0.35	-0.18	0.36	
Etc	0.26	0.23	0.19	0.47	0.45	-0.39	-0.64	-0.77	-0.22	-0.36	0.34	0.34	0.08	-0.35	-0.18	0.48	
Eow	0.22		0.26						-0.26	-0.26	-0.22		0.08	0.09	0.12	0.36	
Al		0.23		0.40	-0.58	-0.86	-0.72	-0.83	-0.35	-0.40	-0.80	-0.77	-0.28	-0.21	-0.20	0.59	
VPD	-0.45	-0.24	0.15	-0.53	0.69	0.87	0.58	0.74		0.38	0.74	0.75	0.63	0.26	-0.09	-0.61	
vch	0.29		0.21		-0.47	-0.63	-0.19	-0.66	-0.29	-0.29	-0.59	-0.42	-0.21	-0.15	0.08	0.54	
vcl	-0.40	-0.16	-0.34		0.35	0.67	0.31	0.68	0.14	0.76	0.66	0.66	-0.18	-0.30	-0.20	-0.50	
Non-ecohydrological variables																	
z		-0.57	-0.32		-0.59			0.20		0.59	-0.48	-0.40	-0.45	-0.10	-0.28	-0.16	-0.35
dzdx	0.17		0.35		-0.29	-0.39		-0.29	0.31	0.22	0.22	-0.13	-0.13	-0.15	0.15	-0.13	-0.34
dzdy	0.18	0.34	0.38	0.15			0.16		0.36	-0.21	-0.20	-0.23	-0.23	-0.16		-0.72	0.43
u10	0.13	0.26	0.26	0.23	0.20	0.38	0.31	0.31	-0.25	-0.20	-0.32	0.16	0.16	0.16		-0.32	
u100	0.13	0.25	0.23	0.23	0.15	0.33	0.25	0.25	-0.27	-0.32	-0.32	0.15	0.15			-0.37	
v10	0.19	0.34			-0.30	-0.34	-0.30	-0.30		-0.34	0.40	0.37				0.35	
v100	0.20	0.28		0.14	-0.40	-0.44	-0.40	-0.40		-0.33	0.45	0.40				0.33	
V		0.25	0.16		-0.33	0.27			-0.43	-0.19	-0.29	0.38	0.38		0.21	0.35	
θ(V)		0.16	0.14	-0.18	-0.24	-0.50	-0.31	-0.31	-0.33	0.33	0.40	0.40	-0.10	-0.10	-0.22	-0.10	0.39
d	-0.47	-0.66	-0.55	-0.40	-0.39		0.25	0.32		0.31	-0.28	-0.25	-0.50	-0.43	-0.57	-0.37	-0.57

Note. The color indicates a positive (red) or negative (blue), and a strong (dark) or weak (light) correlation. Empty cells represent insignificant correlations. Coefficients larger than 0.4 are embolded. tp: total precipitation; te: total evaporation; Evt: evaporation from tree canopy; Ebs: evaporation from bare soil; Etc: evaporation from open water; Eow: evaporation from open water; Al: Aridity index; VPD: vapor pressure deficit; vch: vegetation cover tall vegetation; vcl: vegetation cover short vegetation; z: orography; dzdx: zonal orography gradient; dzdy: meridional orography gradient; u10: zonal wind at 10 m; u100: zonal wind at 100 m; v10: meridional wind at 10 m; v100: meridional wind at 100 m; V: total wind speed; θ(V): wind direction; and d: distance to nearest coast.

variables (Figure S10 and Table S8 in Supporting Information S1). A set is the combination of two variables from which the angle between their loadings $\leq 30^\circ$. None of the ecohydrological variables form a set with any of the non-ecohydrological variables (Figure S10 and Table S8 in Supporting Information S1). For all regions, except central Chile, there are more sets of ecohydrological variables than of non-ecohydrological variables (Text S3 and Tables S3–S7 in Supporting Information S1). Furthermore, on average, there is a stronger clustering among the ecohydrological variables than the non-ecohydrological variables.

Finally, taking into account the results of the PCA and Spearman rank correlation analysis, we observe that variables related to vegetation correlate to ELMR and PLMR across regions. Furthermore, these vegetation-related variables appear to be linked to the hydrological cycle as they cluster with other ecohydrological variables. The dependence of ELMR and PLMR on vegetation related variables also appears to be visible from the relatively large amount of insignificant correlations that ELMR and PLMR have with non-ecohydrological variables for some of the regions, and from the lack of clustering between ecohydrological and non-ecohydrological variables.

4. Discussion

Local moisture recycling has stronger correlations with ecohydrological variables than with non-ecohydrological variables, which indicates that the local water cycle corresponds more strongly to vegetation and the hydrological cycle than to other landscape characteristics. In this study we split up local moisture recycling in local evaporation recycling (ELMR) and local precipitation recycling (PLMR), which we obtained from the output of a dynamical model. The clear statistical relations of ecohydrological variables with ELMR and PLMR may have implications for our understanding of the effect of land cover changes on the local hydroclimate, as the proportion of locally recycled water does not seem to be fixed, but dependent on vegetation itself. This is further supported by our finding that variables that are associated with an increase in vegetation, such as transpiration and evaporation over tree canopy, tend to coincide with a larger fraction of locally recycled water. Furthermore, clustering among the ecohydrological variables suggests that changes in either the water cycle or vegetation could affect local recycling either directly or indirectly through interactions among ecohydrological variables, enhancing the importance of ecohydrological variables for local recycling.

4.1. Patterns in Local Evaporation Recycling and Local Precipitation Recycling

Although ELMR and PLMR are low on average (1%–2%), they vary strongly in space and time. Both ELMR and PLMR peak over elevated regions and during summer. Peaks over mountainous regions can be explained by the orographic lift that pushes air upward over the mountain, which causes the air to cool down and the moisture in it to condensate, forming raindrops (Roe, 2005). In the Mediterranean Basin, maximum ELMR exceeds 5% and maximum PLMR exceeds 30%. These high values are likely caused by the complex topography within the region. Furthermore, ELMR is larger on the Northern Hemisphere than on the Southern Hemisphere (Figure S2a in Supporting Information S1). This may result from the location of the two driest regions, South West Australia and the Cape region of South Africa, on the Southern Hemisphere. There was no clear difference in PLMR between the Northern and Southern Hemisphere, which could be due to differences in the contribution of oceanic moisture sources to tP (Jana et al., 2018) among the Mediterranean regions. Differences between ELMR and PLMR, and how strongly they vary throughout the year, are the result of a mismatch between evaporation and precipitation. This mismatch results from the strong seasonality of precipitation as Mediterranean regions are characterized by wet winters and dry summers. During winter, there is a larger moisture transport from the ocean and sea toward land compared to summer (Batibeniz et al., 2020; Holgate et al., 2020) and during summer, there is a larger contribution of terrestrial moisture sources to precipitation (Gómez-Hernández et al., 2013; Holgate et al., 2020), resulting in smaller PLMR in winter and larger PLMR in summer.

Peaks in evaporation and precipitation recycling over elevated regions and during summer were also found in previous studies at a larger regional scale, for example, for recycling within 150 km (Van der Ent et al., 2010). In addition, continental moisture recycling also peaks during summer (Rios-Entenza et al., 2014; Tuinenburg et al., 2020b; Van der Ent et al., 2010). Earlier findings have shown that the spatial and temporal patterns of ELMR are robust between two models (Theeuwes et al., 2023a). However, the models yielded a different range of values (Theeuwes et al., 2023a), indicating that exact values of ELMR and PLMR should be interpreted and treated more carefully than their patterns. Isotopic ratios have been suggested as proxies for recycling

observations, however, their relationship with atmospheric moisture recycling is complex and needs further investigation (Cropper et al., 2021). Therefore, aside from comparing output from different models, it is currently not possible to validate the outcome of different moisture tracking models.

4.2. Underlying Variables of Local Evaporation Recycling and Local Precipitation Recycling

The ecohydrological variables are more important for ELMR and PLMR than the non-ecohydrological variables in all regions except for central Chile. This anomaly is possibly due to the region's high mountains. For the other four regions overall, we find that precipitation, VPD, and evaporation over tree canopy relate strongly to both ELMR and PLMR. The strong correlations between evaporation over tree canopy and ELMR may be a result of that intercepted water precipitates closer to its source than transpired water (Van der Ent et al., 2014). However, specifically for the Mediterranean Basin, which has the largest transpiration flux of all five regions, we also find positive correlation between ELMR and transpiration during spring, summer, and autumn (Table 1). In addition, for the Mediterranean Basin, PLMR correlates little with either ecohydrological or non-ecohydrological variables, potentially due to a strong contribution of moisture from the Mediterranean Sea. Striking is that tP positively correlates with ELMR and negatively with PLMR. The former holds for all regions and suggests that for Mediterranean-type climate regions, an increase in precipitation may result in a stronger-than-linear increase in the absolute amount of recycled evaporation, as ELMR is a relative metric. This increase in ELMR, and thus precipitation, can feedback to an increase in vegetation, which could result in a positive feedback loop (Chen et al., 2020; Dekker et al., 2007; Spracklen et al., 2012) that strengthens the water cycle.

Even though the results show some clear patterns, they should be interpreted with care and a number of limitations should be considered. First, the Mediterranean regions vary in size, resulting in a different sample size for each region, affecting the statistical outcomes. For instance, smaller sample sizes result in less statistical power, which may explain the large amount of insignificant correlation coefficients for the Cape region of South Africa. However, most important is that the variation in size does not have a direct influence on ELMR and PLMR, as these metrics are calculated over a constant area. To compare recycling of moisture within areas with varying sizes, which is the case for regional recycling, recycling ratios need to be scaled to assess the impact of the region's size. Normalizing ERM and PRM shows that both types of regional recycling do not scale linearly with the region's size, which is probably due to differences in the characteristics of each region specifically, such as shape and topography. Also climate affects regional recycling ratios, as ERM and PRM in Mediterranean regions are smaller than in the tropics (Tuinenburg et al., 2020b).

Naturally, correlation does not imply causality. To overcome this limitation, we suggest as a follow-up to study ELMR and PLMR using regional climate models (e.g., Jach et al., 2020), or simple column models (e.g., Konings et al., 2011), for a more careful assessment of the underlying processes of ELMR and PLMR. The results of our study could inform the design of such a follow-up study, for example, it should explicitly consider the different evaporation fluxes. Our study also did not include all relevant parameters. For example, we did not include any soil characteristics, which affect infiltration (Lehmann et al., 2018; Mayor et al., 2009) and, therefore, affect to what extent an increase in ELMR may feed back to vegetation. Finally, our results show it is possible to identify local scale processes underlying ELMR and PLMR using data with a resolution of 50 km. However, a similar study at an even higher resolution is likely to bring an even more detailed understanding of the underlying local processes.

4.3. Outlook: The Potential and Impact of Land Cover Changes to Enhance Rainfall

The future drying that is projected across Mediterranean regions will probably affect ELMR and PLMR due to their apparent dependency on wetness. We expect ELMR to generally decrease in the future, because ELMR is smaller during dry periods (Theeuwens et al., 2023a). Conversely, we expect PLMR to generally increase due to its negative correlation with wetness. This projected drying could be reduced by greening as it is suggested that greening may enhance rainfall (Griscom et al., 2017; Staal et al., 2024). However, tree restoration may also enhance local drying in regions with little moisture recycling (Hoek van Dijke et al., 2022). Our results suggest that, despite generally low ELMR and PLMR, vegetation increases may enhance both types of local recycling and may initiate a positive feedback. Therefore, greening could contribute to reducing future drying, under the condition that the evaporation increase is compensated for by the increase in precipitation.

ELMR could be used to find locations in each of the five Mediterranean-type climate regions where regreening has a relatively large potential to minimize drying locally. Among locations with such a high regreening potential, PLMR could indicate where an increase in local rainfall has a significant impact; the impact increases with higher PLMR. In regions with a relatively high ELMR and PLMR, regreening may strengthen the local water cycle significantly. However, most evaporation recycles non-locally (Theeuwens et al., 2023a) and, therefore, regreening will likely be more effective on a larger scale.

Although ELMR shows consistent patterns globally with peaks over wet (e.g., tropics) and elevated (e.g., montane grassland) areas and during summer (Theeuwens et al., 2023a), it is unclear if regreening could also strengthen the water cycle in other-climate-type regions, given that even among the Mediterranean regions, there seems to be variation in the underlying processes of ELMR and PLMR. This variation highlights the importance of region-specific characteristics underlying ELMR and PLMR and suggests that land cover changes have a different effect on the local water cycle for each Mediterranean region and likely also other-type-climate regions.

5. Conclusions

We studied moisture recycling on a scale of approximately 50 km for five Mediterranean-type climate regions globally. We looked at local evaporation recycling (ELMR), that is, the fraction of evaporated moisture that returns as precipitation within 50 km from its source, and established its precipitation equivalent: local precipitation recycling (PLMR), that is, the fraction of precipitation that evaporated from within 50 km of where it precipitates. This spatial scale of 50 km allowed us to find the relations of ELMR and PLMR with ecohydrological and non-ecohydrological variables.

Overall, ELMR and PLMR are small (1%–2%), but peak over mountainous regions and during summer. In addition, ELMR peaks over wet regions and PLMR peaks over dry regions. In general, ELMR and PLMR correlate the strongest and most frequently with ecohydrological variables, indicating that the local water cycle is susceptible to land cover changes. This suggests potential to enhance local water availability with climate adaptation measures.

The correlations between ELMR/PLMR and ecohydrological/non-ecohydrological variables vary among the Mediterranean regions. Differences in vegetation, topography and wetness among the regions contribute to these differences. The driest region, South West Australia, has the lowest ELMR. ELMR and PLMR are largest in the Mediterranean Basin, possibly due to its complex topography. In central Chile, our results imply that vegetation and the hydrological cycle have a relatively small impact on ELMR compared to other regions, suggesting that ELMR may be fixed by the high mountains. Finally, differences in vegetation cover and the partitioning of evaporation fluxes among the regions could cause differences in ELMR and PLMR.

As a first step in determining local hydrological impacts of land cover changes, we showed that both ELMR and PLMR are dependent on land cover type. As a next step, region-specific studies are needed to determine if and where land cover changes may enhance rainfall locally. Our results suggest that there mainly is potential for this in mountainous regions and in the Mediterranean-type regions of the Northern Hemisphere, specifically the Mediterranean Basin. Finally, our results suggest that an increase in evaporation due to land cover changes may enhance precipitation and consequently reduce local drying if evaporated losses are compensated for.

Data Availability Statement

The high-resolution atmospheric moisture connections are available at Pangaea (<https://doi.pangaea.de/10.1594/PANGAEA.912710>) (Tuinenburg et al., 2020a). The local evaporation recycling ratio data are freely available at Zenodo <https://doi.org/10.5281/zenodo.7684640> (Theeuwens et al., 2023b). The local precipitation recycling ratio data and regional moisture recycling data are freely available at Zenodo, <http://doi.org/10.5281/zenodo.13868472> (Theeuwens et al., 2024). Scripts that can be used to interpret the moisture recycling ratios are freely available on GitHub, <https://github.com/jtheeu/LocalMoistureRecycling> (Theeuwens, 2024). The Mediterranean mask is published as a supplement to this paper. The ERA5 data is freely available at the Copernicus Climate Change

Service (C3S) Climate Data Store <https://cds.climate.copernicus.eu> (Hersbach et al., 2023). The “Distance to Nearest Coast” dataset is available at <https://oceancolor.gsfc.nasa.gov/docs/distfromcoast/> (NASA, 2012).

Acknowledgments

We wish to thank the reviewers for commenting on earlier versions of this paper. We would like to thank Obbe Tuinenburg for the helpful discussions. This work was performed in the cooperation framework of Wetsus, European Centre of Excellence for Sustainable Water Technology (www.wetsus.eu). Wetsus is co-funded by the Dutch Ministry of Economic Affairs and Climate Policy, the Northern Netherlands Provinces, and the Province of Fryslan. The authors would like to thank the participants of the natural water production theme (DEME and The Weather Makers) for the fruitful discussions and financial support. AS acknowledges support from the Talent Programme Grant VI. Veni.202.170 by the Dutch Research Council (NWO).

References

- Abdi, H., & Williams, L. J. (2010). Principal component analysis. *Wiley Interdisciplinary Reviews: Computational Statistics*, 2(4), 433–459. <https://doi.org/10.1002/wics.101>
- Ali, E., Cramer, W., Carnicer, J., Georgopoulou, E., Hilmi, N. J. M., Le Cozannet, G., & Lionello, P. (2022). Cross-chapter paper 4: Mediterranean region. In *Climate change 2022: Impacts, adaptation and vulnerability. Contribution of working group II to the sixth assessment report of the intergovernmental panel on climate change*. Cambridge University Press. <https://doi.org/10.1017/9781009325844.021.2233>
- Baker, J. C. A. (2021). Planting trees to combat drought. *Nature Geoscience*, 14(7), 458–459. <https://doi.org/10.1038/s41561-021-00787-0>
- Batibenziz, F., Ashfaq, M., Önoel, B., Turuncoglu, U. U., Mehmood, S., & Evans, K. J. (2020). Identification of major moisture sources across the Mediterranean Basin. *Climate Dynamics*, 54(9–10), 4109–4127. <https://doi.org/10.1007/s00382-020-05224-3>
- Bonan, G. B. (2008). Forests and climate change: Forcings, feedbacks, and the climate benefits of forests. *Science*, 320(5882), 1444–1449. <https://doi.org/10.1126/science.1155121>
- Bro, R., & Smilde, A. K. (2014). Principal component analysis. *Analytical Methods*, 6(9), 2812–2831. <https://doi.org/10.1039/c3ay41907j>
- Chen, Z., Wang, W., & Fu, J. (2020). Vegetation response to precipitation anomalies under different climatic and biogeographical conditions in China. *Scientific Reports*, 10(1), 830. <https://doi.org/10.1038/s41598-020-57910-1>
- Cropper, S., Solander, K., Newman, B. D., Tuinenburg, O. A., Staal, A., Theeuwes, J. J. E., & Xu, C. (2021). Comparing deuterium excess to large-scale precipitation recycling models in the tropics. *Npj Climate and Atmospheric Science*, 4(1), 1–9. <https://doi.org/10.1038/s41612-021-00217-3>
- Cui, J., Lian, X., Huntingford, C., Gimeno, L., Wang, T., Ding, J., et al. (2022). Global water availability boosted by vegetation-driven changes in atmospheric moisture transport. *Nature Geoscience*, 15(12), 982–988. <https://doi.org/10.1038/s41561-022-01061-7>
- Dekker, S. C., Rietkerk, M., & Bierkens, M. F. P. (2007). Coupling microscale vegetation-soil water and macroscale vegetation-precipitation feedbacks in semiarid ecosystems. *Global Change Biology*, 13(3), 671–678. <https://doi.org/10.1111/j.1365-2486.2007.01327.x>
- Ellison, D., Wang-Erlandsson, L., van Der Ent, R., & van Noordwijk, M. (2019). Upwind forests: Managing moisture recycling for nature-based resilience. *Unasylva*, 70(251), 14–26.
- Esler, K. J., Jacobsen, A. L., & Pratt, R. B. (2018). *The biology of Mediterranean-type ecosystems* (1st ed.). Oxford University Press. <https://doi.org/10.1093/oso/9780198739135.001.0001>
- Galleguillos, M., Gimeno, F., Puelma, C., Zambrano-Bigiarini, M., Lara, A., & Rojas, M. (2021). Disentangling the effect of future land use strategies and climate change on streamflow in a Mediterranean catchment dominated by tree plantations. *Journal of Hydrology*, 595, 126047. <https://doi.org/10.1016/j.jhydrol.2021.126047>
- Gómez-Hernández, M., Drumond, A., Gimeno, L., & Garcia-Herrera, R. (2013). Variability of moisture sources in the Mediterranean region during the period 1980–2000. *Water Resources Research*, 49(10), 6781–6794. <https://doi.org/10.1002/wrcr.20538>
- Griscom, B. W., Adams, J., Ellis, P. W., Houghton, R. A., Lomax, G., Miteva, D. A., et al. (2017). Natural climate solutions. *Proceedings of the National Academy of Sciences of the United States of America*, 114(44), 11645–11650. <https://doi.org/10.1073/pnas.1710465114>
- Hersbach, H., Bell, B., Berrisford, P., Biavati, G., Horányi, A., Muñoz Sabater, J., et al. (2023). ERA5 monthly averaged data on single levels from 1940 to present [Dataset]. *Copernicus Climate Change Service (C3S) Climate Data Store (CDS)*. <https://doi.org/10.24381/cds.f17050d7>
- Hersbach, H., Bell, B., Berrisford, P., Hirahara, S., Horányi, A., Muñoz-Sabater, J., et al. (2020). The ERA5 global reanalysis. *Quarterly Journal of Royal Meteorological Society*, 146(730), 1999–2049. <https://doi.org/10.1002/qj.3803>
- Hoek van Dijke, A. J., Herold, M., Mallick, K., Benedict, I., Machwitz, M., Schlerf, M., et al. (2022). Shifts in regional water availability due to global tree restoration. *Nature Geoscience*, 15(5), 363–368. <https://doi.org/10.1038/s41561-022-00935-0>
- Holgate, C. M., Evans, J. P., Dijk, I. J. M. V., Pitman, J., & Virgilio, G. D. I. (2020). Australian precipitation recycling and evaporative source regions. *Journal of Climate*, 33(20), 8721–8735. <https://doi.org/10.1175/JCLI-D-19-0926.1>
- Jach, L., Warrach-Sagi, K., Ingwersen, J., Kaas, E., & Wulfmeyer, V. (2020). Land cover impacts on land-atmosphere coupling strength in climate simulations with WRF over Europe. *Journal of Geophysical Research: Atmospheres*, 125(18), e2019JD031989. <https://doi.org/10.1029/2019JD031989>
- Jana, S., Rajagopalan, B., Alexander, M. A., & Ray, A. J. (2018). Understanding the dominant sources and tracks of moisture for summer rainfall in the southwest United States. *Journal of Geophysical Research: Atmospheres*, 123(10), 4850–4870. <https://doi.org/10.1029/2017JD027652>
- Keys, P. W., Van der Ent, R. J., Gordon, L. J., Hoff, H., Nikoli, R., & Savenije, H. H. G. (2012). Analyzing precipitationsheds to understand the vulnerability of rainfall dependent regions. *Biogeosciences*, 9(2), 733–746. <https://doi.org/10.5194/bg-9-733-2012>
- Keys, P. W., Wang-Erlandsson, L., & Gordon, L. J. (2016). Revealing invisible Water: Moisture recycling as an ecosystem service. *PLoS One*, 11(3), e0151993. <https://doi.org/10.1371/journal.pone.0151993>
- Keys, P. W., Wang-Erlandsson, L., Gordon, L. J., Galaz, V., & Ebbesson, J. (2017). Approaching moisture recycling governance. *Global Environmental Change*, 45, 15–23. <https://doi.org/10.1016/j.gloenvcha.2017.04.007>
- Konings, A. G., Dekker, S. C., Rietkerk, M., & Katul, G. G. (2011). Drought sensitivity of patterned vegetation determined by rainfall-land surface feedbacks. *Journal of Geophysical Research*, 116(G4), G04008. <https://doi.org/10.1029/2011JG001748>
- Layton, K., & Ellison, D. (2016). Induced precipitation recycling (IPR): A proposed concept for increasing precipitation through natural vegetation feedback mechanisms. *Ecological Engineering*, 91, 553–565. <https://doi.org/10.1016/j.ecoleng.2016.02.031>
- Lehmann, P., Merlin, O., Gentine, P., & Or, D. (2018). Soil texture effects on surface resistance to bare-soil evaporation. *Geophysical Research Letters*, 45(19), 10398–10405. <https://doi.org/10.1029/2018GL078803>
- Lionello, P., Malanotte-Rizzoli, P., Boscolo, R., Alpert, P., Artale, V., Li, L., et al. (2006). The Mediterranean climate: An overview of the main characteristics and issues. In *Developments in Earth and environmental sciences* (Vol. 4, pp. 1–26). [https://doi.org/10.1016/S1571-9197\(06\)80003-0](https://doi.org/10.1016/S1571-9197(06)80003-0)
- Lu, J., Carbone, G. J., & Grego, J. M. (2019). Uncertainty and hotspots in 21st century projections of agricultural drought from CMIP5 models. *Scientific Reports*, 9(1), 1–12. <https://doi.org/10.1038/s41598-019-41196-z>
- Mayor, Á. G., Bautista, S., & Bellot, J. (2009). Factors and interactions controlling, infiltration, runoff, and soil loss at the microscale in a patchy Mediterranean semiarid landscape. *Earth Surface Processes and Landforms*, 34(12), 1702–1711. <https://doi.org/10.1002/esp.1875>
- Miralles, D. G., Gentine, P., Seneviratne, S. I., & Teuling, A. J. (2019). Land-atmospheric feedbacks during droughts and heatwaves: State of the science and current challenges. *Annals of the New York Academy of Sciences*, 1436(1), 19–35. <https://doi.org/10.1111/nyas.13912>

- Muñoz-Sabater, J., Dutra, E., Agustí-Panareda, A., Albergel, C., Arduini, G., Balsamo, G., et al. (2021). ERA5-Land: A state-of-the-art global reanalysis dataset for land applications. *Earth System Science Data*, 13(9), 4349–4383. <https://doi.org/10.5194/essd-13-4349-2021>
- NASA. (2012). Distance to the nearest coast [Dataset]. <https://oceancolor.gsfc.nasa.gov/docs/distfromcoast/>
- Peel, M. C., Finlayson, B. L., & McMahon, T. A. (2007). Updated world map of the Köppen-Geiger climate classification. *Hydrology and Earth System Sciences*, 11(5), 1633–1644. <https://doi.org/10.5194/hess-11-1633-2007>
- Pranindita, A., Wang-Erlandsson, L., Fetzer, I., & Teuling, A. J. (2022). Moisture recycling and the potential role of forests as moisture source during European heatwaves. *Climate Dynamics*, 58(1–2), 609–624. <https://doi.org/10.1007/s00382-021-05921-7>
- Rios-Entenza, A., Soares, P. M. M., Trigo, R. M., Cardoso, R. M., & Miguez-Macho, G. (2014). Moisture recycling in the Iberian peninsula from a regional climate simulation: Spatiotemporal analysis and impact on the precipitation regime. *Journal of Geophysical Research*, 119(10), 5895–5912. <https://doi.org/10.1002/2013JD021274>
- Roe, G. H. (2005). Orographic precipitation. *Annual Review of Earth and Planetary Sciences*, 33(1), 645–671. <https://doi.org/10.1146/annurev.earth.33.092203.122541>
- Shahidian, S., Serralheiro, R., Serrano, J., Teixeira, J., Haie, N., & Santos, F. (2012). Hargreaves and other reduced-set methods for calculating evapotranspiration. In *Evapotranspiration - Remote sensing and modeling* (pp. 59–80). <https://doi.org/10.5772/18059>
- Spracklen, D. V., Arnold, S. R., & Taylor, C. M. (2012). Observations of increased tropical rainfall preceded by air passage over forests. *Nature*, 489(7415), 282–285. <https://doi.org/10.1038/nature11390>
- Spracklen, D. V., Baker, J. C. A., Garcia-Carreras, L., & Marsham, J. H. (2018). Annual review of environment and resources the effects of tropical vegetation on rainfall. <https://doi.org/10.1146/annurev-environ>
- Staal, A., Theeuwes, J. J. E., Wang-Erlandsson, L., Wunderling, N., & Dekker, S. C. (2024). Targeted rainfall enhancement as an objective of forestation. *Global Change Biology*, 30(1). <https://doi.org/10.1111/gcb.17096>
- Staal, A., Tuinenburg, O. A., Bosmans, J. H. C., Holmgren, M., Van Nes, E. H., Scheffer, M., et al. (2018). Forest-rainfall cascades buffer against drought across the Amazon. *Nature Climate Change*, 8(6), 539–543. <https://doi.org/10.1038/s41558-018-0177-y>
- te Wierik, S. A., Cammeraat, E. L. H., Gupta, J., & Artzy-Randrup, Y. A. (2021). Reviewing the impact of land use and land-use change on moisture recycling and precipitation patterns. *Water Resources Research*, 57(7), e2020WR029234. <https://doi.org/10.1029/2020WR029234>
- Theeuwes, J. (2024). LocalMoistureRecycling [Code]. *GitHub*. Retrieved from <https://github.com/jtheeu/LocalMoistureRecycling>
- Theeuwes, J., Dekker, S. C., Hamelers, B., & Staal, A. (2024). Atmospheric moisture recycling in Mediterranean-type climate regions across the world [Dataset]. *Zenodo*. <https://doi.org/10.5281/zenodo.13868473>
- Theeuwes, J. J. E., Staal, A., Tuinenburg, O. A., Hamelers, B. V. M., & Dekker, S. C. (2023a). Local moisture recycling across the globe. *Hydrology and Earth System Sciences*, 27(7), 1457–1476. <https://doi.org/10.5194/hess-27-1457-2023>
- Theeuwes, J. J. E., Staal, A., Tuinenburg, O. A., Hamelers, B. V. M., & Dekker, S. C. (2023b). Local moisture recycling across the globe [Dataset]. *Zenodo*, 27(7), 1457–1476. <https://doi.org/10.5281/zenodo.7684640>
- Tuinenburg, O. A., Bosmans, J. H. C., & Staal, A. (2022). The global potential of forest restoration for drought mitigation. *Environmental Research Letters*, 17(3), 034045. <https://doi.org/10.1088/1748-9326/ac55b8>
- Tuinenburg, O. A., Hutjes, R. W. A., & Kabat, P. (2012). The fate of evaporated water from the Ganges basin. *Journal of Geophysical Research*, 117(1), 1–17. <https://doi.org/10.1029/2011JD016221>
- Tuinenburg, O. A., & Staal, A. (2020). Tracking the global flows of atmospheric moisture and associated uncertainties. *Hydrology and Earth System Sciences*, 24(5), 2419–2435. <https://doi.org/10.5194/hess-24-2419-2020>
- Tuinenburg, O. A., Theeuwes, J. J. E., & Staal, A. (2020a). Global evaporation to precipitation flows obtained with Lagrangian atmospheric moisture tracking [Dataset]. *PANGAEA*. <https://doi.org/10.1594/PANGAEA.912710>
- Tuinenburg, O. A., Theeuwes, J. J. E., & Staal, A. (2020b). High-resolution global atmospheric moisture connections from evaporation to precipitation. *Earth System Science Data*, 12(4), 3177–3188. <https://doi.org/10.5194/essd-12-3177-2020>
- Van der Ent, R. J., Savenije, H. H. G., Schaeffli, B., & Steele-Dunne, S. C. (2010). Origin and fate of atmospheric moisture over continents. *Water Resources Research*, 46(9), W09525. <https://doi.org/10.1029/2010WR009127>
- Van der Ent, R. J., Wang-Erlandsson, L., Keys, P. W., & Savenije, H. H. G. (2014). Contrasting roles of interception and transpiration in the hydrological cycle - Part 2: Moisture recycling. *Earth System Dynamics*, 5(2), 471–489. <https://doi.org/10.5194/esd-5-471-2014>
- Vautard, R., Cattiaux, J., Yiou, P., Thépaut, J. N., & Ciais, P. (2010). Northern Hemisphere atmospheric stilling partly attributed to an increase in surface roughness. *Nature Geoscience*, 3(11), 756–761. <https://doi.org/10.1038/ngeo979>
- Wang-Erlandsson, L., Fetzer, I., Keys, P. W., van der Ent, R. J., Savenije, H. H. G., & Gordon, L. J. (2018). Remote land use impacts on river flows through atmospheric teleconnections. *Hydrology and Earth System Sciences*, 22(8), 4311–4328. <https://doi.org/10.5194/hess-22-4311-2018>
- Zurbenko, I., & Luo, M. (2015). Surface humidity changes in different temporal scales. *American Journal of Climate Change*, 04(03), 226–238. <https://doi.org/10.4236/ajcc.2015.43018>